

# Status Report on Weak Matrix Element Calculations\*

Rajan Gupta and Tanmoy Bhattacharya <sup>a</sup>

<sup>a</sup>T-8 Group, MS B285, Los Alamos National Laboratory, Los Alamos, New Mexico 87545 U. S. A.

This talk presents results of weak matrix elements calculated from simulations done on  $170\ 32^3 \times 64$  lattices at  $\beta = 6.0$  using quenched Wilson fermions. We discuss the extraction of pseudoscalar decay constants  $f_\pi$ ,  $f_K$ ,  $f_D$ , and  $f_{D_s}$ , the form-factors for the rare decay  $B \rightarrow K^* \gamma$ , and the matrix elements of the 4-fermion operators relevant to  $B_K$ ,  $B_7$ ,  $B_8$ . We present an analysis of the various sources of systematic errors, and show that these are now much larger than the statistical errors for each of these observables. Our main results are  $f_D = 186(29)$  MeV,  $f_{D_s} = 224(16)$  MeV,  $T_1 = T_2 = 0.24(1)$ ,  $B_K(NDR, 2\text{ GeV}) = 0.67(9)$ , and  $B_8(NDR, 2\text{ GeV}) = 0.81(1)$ .

## 1. TECHNICAL DETAILS

We briefly state the details common to all three quantities discussed in this talk and refer the reader to [1–3] for details. Preliminary results based on 100 lattices were presented at LATTICE94 [4] and the final analysis will be presented elsewhere [2,5].

We calculate wall and Wuppertal source quark propagators at five values of quark mass given by  $\kappa = 0.135$  ( $C$ ),  $0.153$  ( $S$ ),  $0.155$  ( $U_1$ ),  $0.1558$  ( $U_2$ ), and  $0.1563$  ( $U_3$ ). These quarks correspond to pseudoscalar mesons of mass 2835, 983, 690, 545 and 431 MeV respectively where we have used  $1/a = 2.33$  GeV for the lattice scale. We construct three types of correlation functions, Wuppertal smeared-local ( $\Gamma_{SL}$ ) and smeared-smeared ( $\Gamma_{SS}$ ), and wall smeared-local ( $\Gamma_{WL}$ ). The three  $U_i$  quarks allow us to extrapolate the data to the physical isospin symmetric light quark mass  $\overline{m} = (m_u + m_d)/2$ , while the physical charm mass is taken to be  $C$ . The physical value of strange quark lies between  $S$  and  $U_1$  and we use these two points to interpolate to it. For brevity we will denote the six combinations of light quarks  $U_1U_1$ ,  $U_1U_2$ ,  $U_1U_3$ ,  $U_2U_2$ ,  $U_2U_3$ ,  $U_3U_3$  by  $\{U_iU_j\}$  and the three degenerate cases by  $\{U_iU_i\}$ . The  $\Gamma_{SL}$ ,  $\Gamma_{SS}$ , and 3-point functions have been evaluated at the 5 lowest lattice momenta, *i.e.*  $p = (0, 0, 0)$ ,  $(1, 0, 0)$ ,  $(1, 1, 0)$ ,  $(1, 1, 1)$ ,  $(2, 0, 0)$ .

\*Based on talks presented by Rajan Gupta and Tanmoy Bhattacharya. These calculations have been done on the CM5 at LANL as part of the DOE HPC Grand Challenge program, and at NCSA under a Metacenter allocation.

**Renormalization Constants:** We use the Lepage-Mackenzie tadpole subtraction prescription [6]. Its implementation consists of three parts in addition to writing the perturbative expansions in terms of the improved coupling  $\alpha_v$ . One, the renormalization of the quark field  $\sqrt{Z_\psi}$  changes from  $\sqrt{2\kappa} \rightarrow \sqrt{8\kappa_c} \sqrt{1 - 3\kappa/4\kappa_c}$ ; second, the perturbative expression for  $8\kappa_c$  in  $Z_\psi$  is combined with the coefficient of  $\alpha_v$  in the one loop matching relations to remove the tadpole contribution, and finally the typical momentum scale once the tadpole diagrams are removed is taken to be  $q^* = 1/a$ , *i.e.* both the scale at which  $\alpha_v$  is evaluated and the scale at which lattice and continuum theories are matched is set to  $q^* = 1/a$ . We label this scheme *TAD1* for brevity. The difference in results for  $q^* = 1/a$  and  $q^* = \pi/a$  is used as an estimate of systematic errors due to fixing  $q^*$ . Our data gives  $\kappa_c = 0.157131(9)$  [1].

**Setting the quark masses:** In [1] we show that a non-perturbative estimate of quark mass  $m_{np}$ , calculated using the Ward identity, is linearly related to  $(1/2\kappa - 1/2\kappa_c)$  for light quarks, so either definition of the quark mass can be used for the extrapolation. We choose to use  $m_{np}$ , and fix  $\overline{m}$ ,  $m_s$  and  $m_c$  as follows. To get  $\overline{m}$  we extrapolate the ratio  $M_\pi^2/M_\rho^2$  to its physical value 0.03182. We determine  $m_s$  by extrapolating  $M_\phi/M_\rho$  to  $\overline{m}$  and then interpolating in the strange quark to match the physical value. We find a  $\sim 20\%$  difference between using  $M_K^2/M_\pi^2$  or  $M_\phi/M_\rho$  to fix  $m_s$ , which we use as an estimate of the systematic error. For  $m_c$  we use  $\kappa = 0.135$  as we

have simulated only one heavy mass. With this choice the experimental values of  $M_D$ ,  $M_{D^*}$  and  $M_{D_s}$  lie in between the static mass  $M_1$  (measured from the rate of exponential fall-off of the 2-point function) and the kinetic mass defined as  $M_2 \equiv (\partial^2 E / \partial p^2 |_{p=0})^{-1}$ . The difference in final quantities between using  $M_1$  and  $M_2$  is taken to be an estimate of the systematic error in fixing  $m_c$ .

**The lattice scale  $a$ :** To convert lattice results to physical units we use  $a(M_\rho)$ . As discussed in [1], the  $M_\rho$  data show a small but statistically significant negative curvature. We get  $1/a = 2.330(41)$  GeV from a linear fit to  $\{U_i U_j\}$  points,  $2.365(48)$  GeV including a  $m^{3/2}$  correction term in the fit to the 10  $U_i U_j, SU_i, SS$  points, and  $2.344(42)$  GeV including a  $m^2$  term. Since all three estimates are consistent and the form of the chiral correction cannot be resolved we use the result from the linear extrapolation and assign 3% as an estimate of the systematic error.

## 2. DECAY CONSTANTS

The pseudoscalar decay constant  $f_{PS}$  is given by

$$f_\pi = \frac{Z_A \langle 0 | A_4^{\text{local}} | \pi(\vec{p}) \rangle}{E_\pi(\vec{p})}, \quad (1)$$

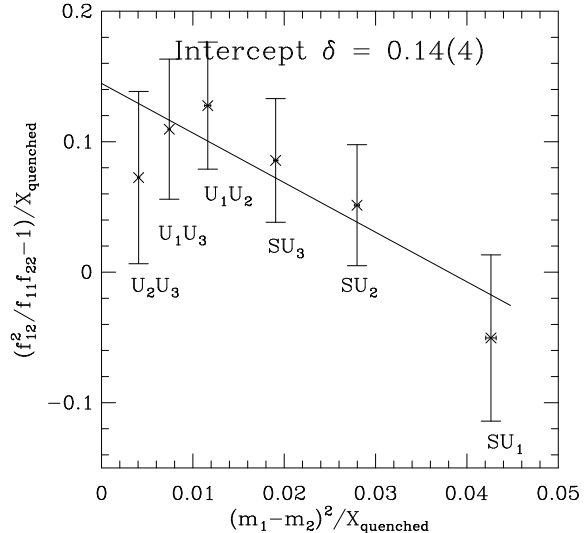
where  $Z_A$  is the renormalization constant connecting the lattice scheme to continuum  $\overline{MS}$ . We study, in addition to the 2-point correlation functions  $\Gamma$ , two kinds of ratios of correlators:

$$R_1(t) = \frac{\Gamma_{SL}(t)}{\Gamma_{SS}(t)}; \quad R_2(t) = \frac{\Gamma_{SL}(t)\Gamma_{SL}(t)}{\Gamma_{SS}(t)}. \quad (2)$$

Using either  $\pi$  or  $A_4$  for the smeared source  $J$  gives 4 ways of extracting  $f_{PS}$ . Two more ways are gotten by combining the mass and amplitude of the 2-point correlation functions, *i.e.*  $\langle A_4 P \rangle_{LS}$  and  $\langle PP \rangle_{SS}$ , and  $\langle A_4 A_4 \rangle_{LS}$  and  $\langle A_4 A_4 \rangle_{SS}$ .

The data satisfy the following consistency checks: the six ways of calculating  $f_{PS}$  described above, and at each of the five values of momentum, give results consistent to within  $2\sigma$  [2]. (The one exception is the  $\vec{p} = (2, 0, 0)$  case where the signal is not good enough to ascertain that we have fit to the lowest state.) Even though these

Figure 1. Plot of the Bernard-Golterman ratio  $R$  for the quenched theory.

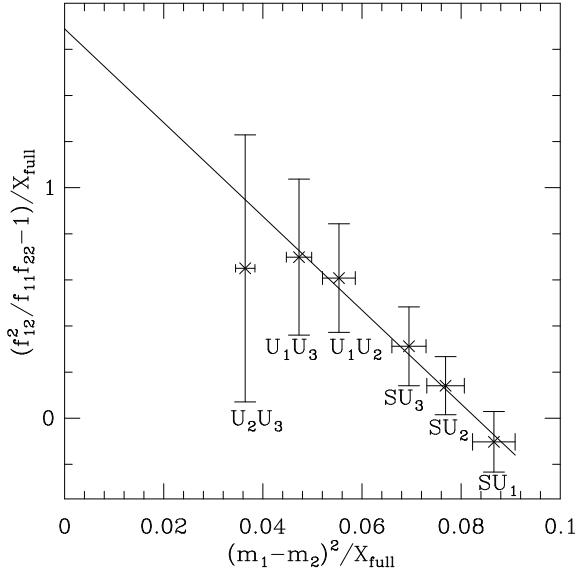


estimates are correlated, consistent results do indicate that fits have been made to the lowest state and reassure us of the statistical quality of the data. We use the  $\vec{p} = (0, 0, 0)$  data in our final analysis as it has the best signal.

**Quenched approximation** When analyzed in terms of chiral perturbation theory (CPT), there are two consequences of using the quenched approximation. One, the coefficients in the quenched theory are different from those in full QCD and uncalculable, and second, Sharpe and collaborators [7] and Bernard and Golterman [8] have pointed out that there exist extra chiral logs due to the  $\eta'$  as it is also a Goldstone boson in the quenched approximation. These make the chiral limit of quenched quantities sick. To analyze the effects of  $\eta'$  loops Bernard and Golterman [8] have constructed the ratio  $R \equiv f_{12}^2 / f_{11} f_{22}$  applicable in a 4-flavor theory where  $m_1 = m_{1'}$  and  $m_2 = m_{2'}$ . The advantages of this ratio in comparing full and quenched theories is that it is free of ambiguities due to the cutoff  $\Lambda$  in loop integrals and  $O(p^4)$  terms in the chiral Lagrangian. CPT predicts that

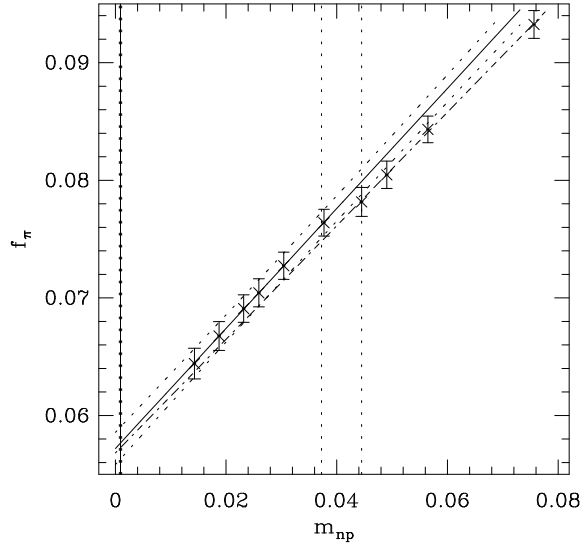
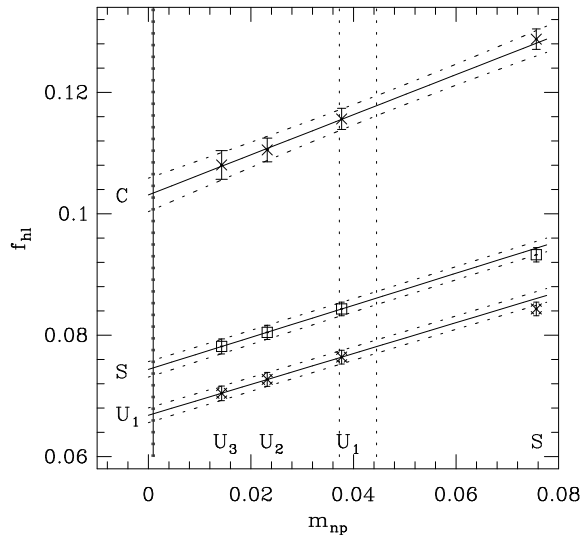
$$R^Q - 1 = \delta X_{\text{quenched}} + O((m_1 - m_2)^2)$$

$$R^F - 1 = X_{\text{full}} + O((m_1 - m_2)^2)$$

Figure 2. Plot of  $R$  for the full theory.

where  $\delta \equiv m_0^2 / 24\pi^2 f_\pi^2$  parameterizes the effects of the  $\eta'$ , and  $X_{quenched}$  and  $X_{full}$  are given in [9]. At LATTICE94 the preferred fit (with 100 configurations and no  $(m_1 - m_2)^2$  term) was to the quenched expression which gave  $\delta = 0.10(3)$  [9]. The need for including the  $(m_1 - m_2)^2$  correction is shown in Figs. 1 and 2. The fit to the quenched expression gives  $\delta = 0.14(4)$ , however, based on  $\chi^2$ , the fit to the full QCD expression is preferred. The caveat is that the intercept is 1.69(45) rather than unity. Thus, we cannot resolve the effects of  $\eta'$  from normal higher order terms in the chiral expansion, and neglect both in our analysis.

**Extrapolation to the physical quark masses:** The data, shown in Fig. 3, indicates a break in the vicinity of  $m_s$  between the non-degenerate  $\{SU_i\}$  and degenerate  $U_1U_1$  mesons at the  $1\sigma$  level, but no such break between the  $U_1U_i$  and the  $U_2U_2$  cases. We thus use  $\{U_iU_j\}$  points to extrapolate to  $f_\pi$ . Note that even though the slopes for the two fits to  $\{U_iU_j\}$  and  $\{SS, SU_i\}$  combinations are different, the values after extrapolation are virtually indistinguishable. In Fig. 4 we show the extrapolation for heavy-light mesons for three cases ( $C$ ,  $S$ ,  $U_1$ ) of “heavy” quarks. In all three cases we use a linear fit to the three  $U_i$  points for extrapolation to  $\bar{m}$  as deviations from linearity are apparent if the “light”

Figure 3. Plot of data for  $f_\pi$  versus  $m_{np}$ . The linear fit (solid line) is to the six  $\{U_iU_j\}$  points, with errors shown by the dotted lines. The dash-dot line is a linear fit to the four  $\{SS, SU_i\}$  points. The vertical line at  $m_{np} \approx 0$  represents  $\bar{m}$  and the band at  $m_{np} \approx 0.04$  denotes the range of  $m_s$ .Figure 4. Extrapolation of heavy-light  $f_{PS}$  to  $\bar{m}$  for three cases,  $C$ ,  $S$ ,  $U_1$ , of “heavy” quarks. The linear fits are to the three “light”  $U_i$  quarks, and the fourth point (light quark is  $S$ ) is included to show the breakdown of the linear approximation.

quark mass is taken to be  $S$  as shown by the fourth point at  $m_{np} = 0.076$ . To get  $f_K$  we interpolate to  $m_s$  the result of the extrapolations of  $SU_i$  and  $U_1U_i$  points to  $\bar{m}$ . For  $f_D$  we extrapolate the three  $CU_i$ , and for  $f_{D_s}$  we simply interpolate between  $CU_1$  and  $CS$  points.

**Results at  $\beta = 6.0$ :** Our final results using  $TAD1$  scheme along with estimates of statistical and various systematic errors are given in Table 1. From the data it is clear that systematic errors due to setting  $m_c$ , the lattice scale, and  $Z_A$  are now the dominant sources of errors.

**Continuum Limit:** To extract results valid in the continuum limit we include data from the GF11 ( $\beta = 5.7, 5.93, 6.17$ ) [10], JLQCD ( $\beta = 6.1, 6.3$ ) [12], and APE ( $\beta = 6.0, 6.2$ ) [11] Collaborations. We have attempted to correct for as many systematic differences, however some, like differences in lattice volumes, range of quark masses analyzed, and fitting techniques, remain.

Assuming that lattice spacing errors are  $O(a)$ , a linear fit versus  $M_\rho a$  gives

$$\begin{aligned} f_\pi/M_\rho &= 0.156(7) & (\text{expt. } 0.170), \\ f_K/M_\rho &= 0.171(6) & (\text{expt. } 0.208). \end{aligned}$$

with  $\chi^2/dof = 1.6$  and  $1.7$  respectively. The change from the GF11 results is marginal as the fit is still strongly influenced by the point at  $\beta = 5.7$ , which may lie outside the domain of validity of the linear extrapolation. A linear extrapolation excluding the  $\beta = 5.7$  data gives

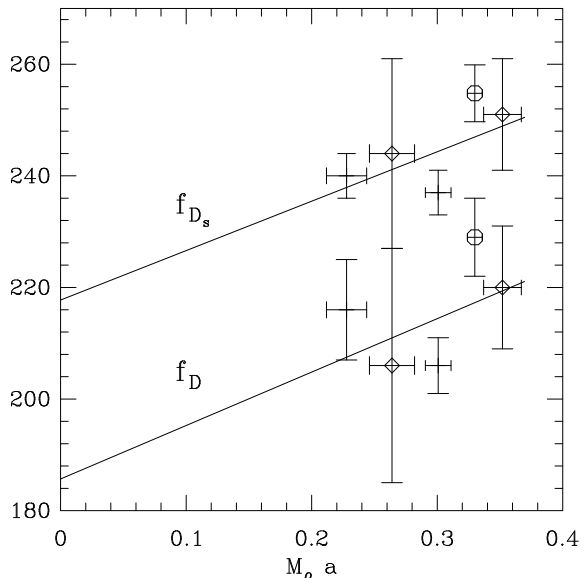
$$f_\pi/M_\rho = 0.170(14), \quad f_K/M_\rho = 0.187(11),$$

with  $\chi^2/dof = 2.1$  and  $1.9$  respectively. Using  $m_s(M_\phi)$  would increase  $f_K$  by  $\sim 2\%$ . Given this difference in the extrapolated value depending on whether the data at  $\beta = 5.7$  is included or not makes it clear that more data are required to make a reliable  $a \rightarrow 0$  extrapolation.

The  $f_D$  and  $f_{D_s}$  data at  $\beta \geq 6.0$ , in  $TAD1$  scheme, and using  $m_s(M_K)$  are shown in Fig. 5. The APE collaboration use  $M_1$  for the meson mass. For consistency we have shifted their data to  $M_2$  using our estimates given in Table 1. A linear extrapolation to  $a = 0$  then gives

$$f_D = 186(29) \text{ MeV}, \quad f_{D_s} = 218(15) \text{ MeV},$$

Figure 5. Extrapolation to the continuum limit of  $f_D$  and  $f_{D_s}$  (in MeV) data. Our data is shown with the symbol octagon, the plus points are from the JLQCD Collaboration [12], and the diamonds label the APE collaboration [11] data.



with  $\chi^2/dof = 2.2$  and  $2.0$  respectively. Using  $m_s(M_\phi)$  increases  $f_{D_s}$  to  $224(16)$  MeV. The quality of the fits are, however, not very satisfactory. The bottom line is that in order to improve the estimates the various systematic errors that have not been included in the  $a \rightarrow 0$  extrapolations presented above need to be reduced.

### 3. THE RARE DECAY $B \rightarrow K^*\gamma$ .

We discuss the applicability of heavy quark effective theory (HQET) and pole dominance hypothesis (PDH) to extract the form-factors  $T_1$  and  $T_2$  at  $Q^2 = 0$  and  $m_{heavy} = m_b$ . The technical setup is the same as described in [3] for the calculation of semi-leptonic form-factors, and the quality of the signal is similar to that for  $D \rightarrow K^*l\nu$  decays.

**PDH:** states that the  $Q^2$  behavior of all form-factors is

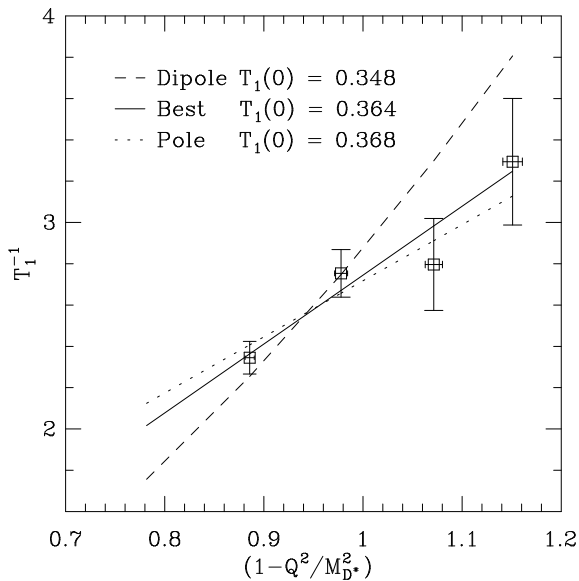
$$f(Q^2) = f(0)/(1 - Q^2/M^2), \quad (3)$$

where  $M$  is the mass of the nearest resonance with the right quantum numbers. To test PDH

Table 1. Our final results at  $\beta = 6.0$ . All dimensionful numbers are given in  $MeV$  with the scale set by  $M_\rho$ . For the systematic errors due to  $m_s$ ,  $m_c$ ,  $q^*$  we also give the sign of the effect. We cannot estimate the uncertainty due to using the quenched approximation, or for entries marked with a ?.

	Best Estimate	Statistical & Extrapolation	Tuning $m_s$	Tuning $m_c$	$q^*$	Tuning $a$ (3%)	$Z_A$
$f_\pi$	134	4	—	—	+2	4	10
$f_K$	159	3	-3	—	+3	5	10
$f_D$	229	7	—	+12	+4	7	14
$f_{D_s}$	260	4	-5	+15	+4	8	20
$f_K/f_\pi$	1.19	0.02	-0.025	—	—	—	0
$f_D/f_\pi$	1.71	0.05	—	+0.09	—	—	?
$f_{D_s}/f_D$	1.135	0.021	-0.023	+0.006	—	—	0

Figure 6. Three types of fits to test  $Q^2$  behavior of  $T_1$  using  $CU_3 \rightarrow U_1U_3$  transition. HQET suggests a dipole fit if one assumes PDH for  $T_2$ . The data prefer a pole fit but with the resonance mass smaller than the lattice measured value  $M_{D^*}$  used to plot the data.

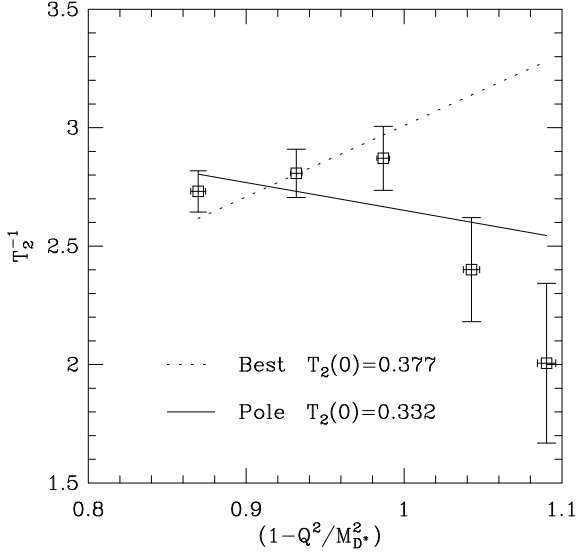
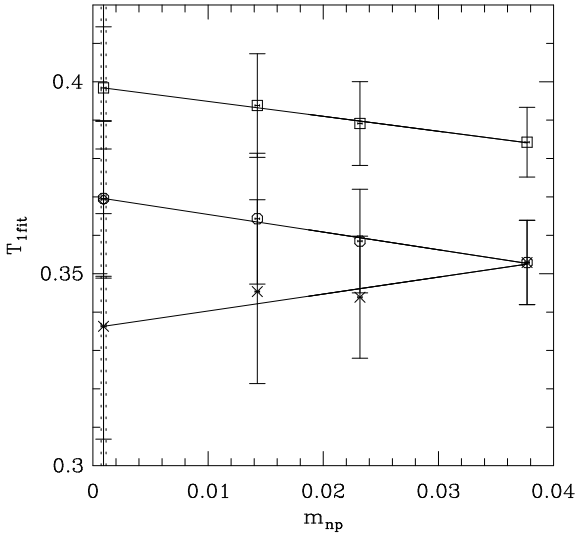
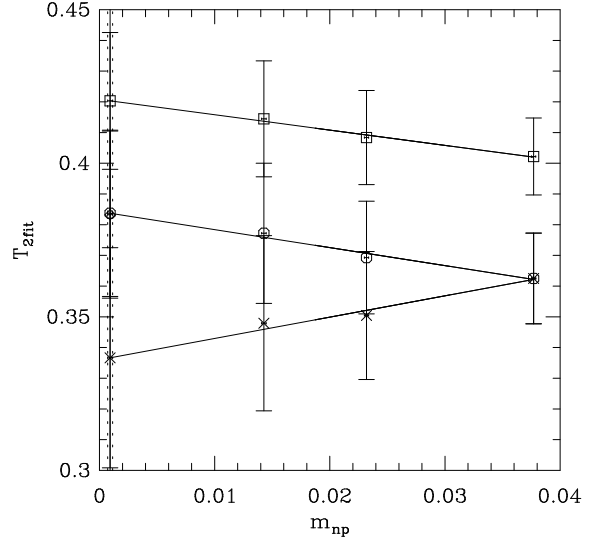


we make two kinds of fits: (i) single parameter “pole” fit where  $M$  is the lattice measured value of the resonance mass, (ii) two parameter “best” fit where  $M$  and  $f(0)$  are free parameters. Typical examples of these fits are shown in Figs. 6 and 7. Overall,  $T_1$  is well described by the “pole” form, whereas  $T_2$  has a “flat”  $Q^2$  dependence. We take the “best” fit values for our final estimates. **HQET:** To leading order in  $\alpha_s$  and in the mass of the heavy quarks, HQET implies (for heavy to heavy transitions) that the combinations

$$\frac{\sqrt{m_B m_{K^*}}}{m_B + m_{K^*}^*} T_1(Q^2) = \frac{\sqrt{m_B m_{K^*}}}{m_B + m_{K^*}^*} \frac{T_2(Q^2)}{1 - \frac{Q^2}{(m_B + m_{K^*}^*)^2}} \quad (4)$$

are independent of the masses of the heavy quarks for fixed velocity transfer. Since  $T_1(Q^2 = 0) = T_2(Q^2 = 0)$  for all  $m_q$ , this HQET relation and the PDH, Eq. 3, cannot hold simultaneously. In fact, for heavy quarks  $(m_B + m_{K^*}) \approx m_{pole}$ , therefore, if  $T_2$  fits the pole form then  $T_1$  must be a ‘dipole’. Instead our data, as exemplified in Figs. 6 and 7, prefer a flat  $T_2$  and a pole behavior for  $T_1$ .

**Dependence on quark mass:** Figures 8 and 9 show examples of the variation of  $T_1(0)$  and  $T_2(0)$  with quark masses. There is significant dependence on the mass of the quark  $C$  decays into (which is a kinematic effect), and a slight dependence on  $m_{spectator}$  resulting in the small increase in slope between  $CU_i \rightarrow U_1U_i$  and  $CU_i \rightarrow SU_i$  cases, which is consistent with HQET.

Figure 7. Fits to test  $Q^2$  behavior of  $T_2$ .Figure 8. Extrapolation of  $T_1(Q^2 = 0)$  to  $m_u$ . The interpolation to  $m_s$  for  $T_1(B \rightarrow K^*\gamma)$  is done using the points labeled by squares ( $s = S$ ) and octagons ( $s = U_1$ ), while  $T_1(B \rightarrow \rho\gamma)$  is obtained by extrapolating the degenerate  $q\bar{q}$  points (crosses).Figure 9. Extrapolation of  $T_2(Q^2 = 0)$  to  $m_u$ . The interpolation to  $m_s$  for  $T_2(B \rightarrow K^*\gamma)$  is done using the points labeled by squares ( $s = S$ ) and octagons ( $s = U_1$ ), while  $T_2(B \rightarrow \rho\gamma)$  is obtained by extrapolating the degenerate  $q\bar{q}$  points (crosses).Table 2. Estimates of form factors in 3 commonly used renormalization schemes defined in [2]. The data satisfy  $T_1(Q^2 = 0) = T_2(Q^2 = 0)$ . The last four rows give  $T(Q^2 = 0)$  extrapolated to  $m_b$  using the 4 methods discussed in the text.

	TAD1	TAD $\pi$	TADU $_0$
$T_1$	0.37(2)	0.39(2)	0.35(2)
$T_2$	0.39(3)	0.40(3)	0.36(2)
(1)	0.097(2)	0.100(2)	0.091(2)
(2)	0.234(8)	0.240(8)	0.218(8)
(3)	0.084(6)	0.086(6)	0.078(5)
(4)	0.236(12)	0.242(13)	0.220(11)

Table 3. Estimates in  $TAD1$  scheme at  $Q^2 = 0$ . The variations give estimates of systematic errors.

		Pole		Best	
		$m_s(M_K)$	$m_s(M_\phi)$	$m_s(M_K)$	$m_s(M_\phi)$
$T_1$	$m_1$	0.37(2)	0.38(2)	0.37(2)	0.37(2)
	$m_2$	0.37(2)	0.38(2)	0.37(2)	0.37(2)
$T_2$	$m_1$	0.33(1)	0.34(1)	0.38(3)	0.39(3)
	$m_2$	0.33(1)	0.34(1)	0.38(3)	0.39(3)
(1)	$m_1$			0.096(2)	0.097(2)
	$m_2$			0.100(2)	0.101(2)
(2)	$m_1$			0.230(8)	0.234(8)
	$m_2$			0.239(9)	0.243(9)
(3)	$m_1$			0.082(6)	0.084(6)
	$m_2$			0.095(6)	0.096(6)
(4)	$m_1$			0.232(13)	0.236(12)
	$m_2$			0.242(13)	0.245(13)

**Extrapolation in  $m_{heavy}$ :** The need to extrapolate the results obtained at  $m_{heavy} \approx m_c$  to  $m_b$  using HQET, Eq. 4, introduces a very large uncertainty as shown by the four ways of analyzing the data. Methods 1 and 2: we take the value of  $T_2$  at zero recoil extrapolated to  $m_s$  and  $\overline{m}$  and scale it to  $m_b$  using HQET. We can then estimate the value at  $Q^2 = 0$  assuming pole dominance holds for  $T_2$  at  $m_b$  (advocated by A. Soni at this conference), or by using a “flat” behavior as shown by data at  $m_{heavy} = m_c$ . Method 3 (4): Scale  $T_2(Q^2 = 0)$  ( $T_1$ ) assuming the joint validity of HQET and pole dominance. This implies the scaling relations  $T_2(Q^2 = 0)m_{heavy}^{3/2} = constant$  and  $T_1(Q^2 = 0)m_{heavy}^{1/2} = constant$ . The results along with their variation with the tadpole subtraction prescription, type of fit,  $m_s$ , and the definition of heavy-light meson mass ( $M_1$  or  $M_2$ ) are shown in tables 2 and 3.

**Results at  $\beta = 6.0$ :** Methods 1,2 and 3,4 reflect the same contradiction. The value is either 0.08 – 0.1 or 0.23 – 0.25 depending on what we assume for the scaling behavior. With present data we assume that the flat  $Q^2$  behavior for  $T_2$  and pole dominance for  $T_1$  persists all the way upto the physical value of  $m_b$ . Then, using the best fit, TAD1 subtraction prescription,  $m_s(M_\phi)$ , and  $M_1$  for the meson mass, we get  $T_1 = T_2 = 0.24(1)$ . Further progress requires clarification of the  $Q^2$  behaviour of the form factors and an estimate of

the violations of leading order HQET predictions.

#### 4. B-parameters

We present an update on results for  $B_K$ ,  $B_7$ ,  $B_8$  with Wilson fermions evaluated in the NDR scheme with  $TAD1$  subtraction prescription. Note that both  $q^*$  and the matching scale between the lattice and continuum theories are taken to be  $1/a$ . Thereafter, the results are run to 2 GeV using the 2-loop relations, however the change is minimal.

To analyze the lattice data (illustrated in Table 4) we consider the general form, ignoring chiral logs, of the chiral expansion of the  $\Delta S = 2$  4-fermion matrix elements with Wilson fermions

$$\begin{aligned} \langle \overline{K^0} | \mathcal{O}_{LL} | K^0 \rangle = & \alpha + \beta m_K^2 + \gamma p_i p_f + \delta_1 m_K^4 \\ & + \delta_2 m_K^2 p_i p_f + \delta_3 (p_i p_f)^2 + \dots \end{aligned} \quad (5)$$

This follows from Lorentz symmetry as  $m^2$  and  $p_i \cdot p_f$  are the only invariants.

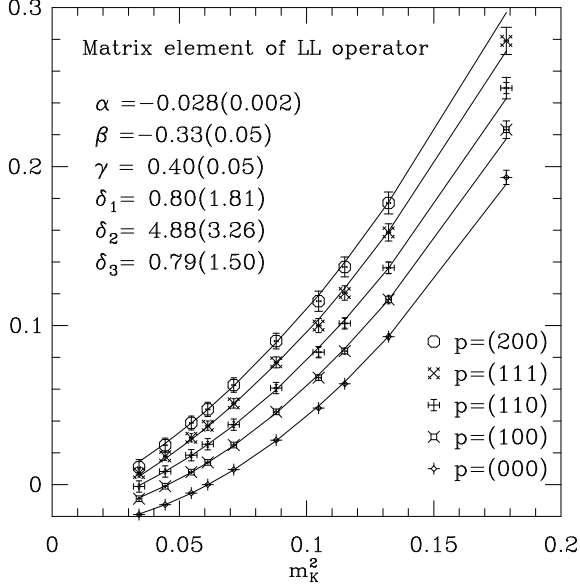
**$B_K$ :** The terms proportional to  $\alpha, \beta$  and  $\delta_1$  are pure lattice artifacts due to mixing of the  $\Delta S = 2$  4-fermion operator with wrong chirality operators. To isolate these terms we fit the data for the lightest 10 mass combinations and for the 5 values of momentum transfer using Eq. 5 as shown in Fig. 10. (Similar values for the six coefficients are obtained from fits to the 6 lightest combinations.) We find that the three  $\delta_i$  are not well determined; only  $\delta_2$  is significantly different from zero. More important, the coefficients  $\gamma, \delta_2, \delta_3$  contain artifacts in addition to the desired physical pieces which we cannot resolve by this method. We simply assume that the 1-loop improved operator does a sufficiently good job of removing these residual artifacts. The result then is

$$B_K(NDR, 1/a) = \gamma + (\delta_2 + \delta_3)M_K^2 = 0.65(10).$$

A second way of extracting  $B_K$  using Eq. 5 is to combine pairs of points at different momentum transfer:

$$\begin{aligned} (E_1 B_K(q_1) - E_2 B_K(q_2)) / (E_1 - E_2) = \\ \gamma + \delta_2 m^2 + \delta_3 m(E_1 + E_2). \end{aligned}$$

This procedure directly removes  $\alpha, \beta$  and  $\delta_1$  but requires a correction to the  $\delta_3 m(E_1 + E_2)$  piece,

Figure 10. Six parameter fit to the  $B_K$  data.

for which we use the value of  $\delta_3$  extracted from the fit. The results of this analysis for the 10 light mass combinations are given in the third column of Table 4. Interpolating to  $m_K$ , we get  $B_K(NDR, 1/a) = 0.66(9)$ .

$\hat{B}_K$ : The 2-loop running of  $B_K$  defines the renormalization group invariant quantity  $\hat{B}_K$  [15]

$$\hat{B}_K = \alpha_s(\mu)^{-2/\beta_0} (1 + \alpha_s(\mu)J/4\pi) B_K(\mu)$$

where  $J = (\beta_1\gamma_0 - \beta_0\gamma_1)/2\beta_0^2 = 2.004$  for  $n_f = 0$ . Under running,  $B_K$  increases as  $\mu$  is decreased. Thus  $B_K(NDR, 1/a) = 0.66(9)$  becomes  $B_K(NDR, 2 \text{ GeV}) = 0.67(9)$ , and  $\hat{B}_K$  is  $0.90(14)$ . For comparison, the Staggered value calculated at  $\beta = 6.0$  is  $B_K(NDR, 2 \text{ GeV}) = 0.67 - 0.71$  depending on the lattice operators used [13,14]. An update on staggered results and issues of extrapolation to  $a \rightarrow 0$  have been presented by JLQCD at this conference [14].

$B_D$ : The  $CS$ ,  $CU_i$  data show no significant variation with momentum transfer as shown in Table 4. The theoretical analysis of artifacts in heavy-light mesons has not yet been completed; indications are that all 6 terms contribute. Therefore we simply extrapolate the  $CU_i$  data to  $\bar{m}$  to get  $B_D(NDR, 1/a) = 0.78(1)$  or  $B_D(NDR, 2 \text{ GeV}) = 0.79(1)$ .

Table 4.  $B_K$ ,  $B_7$  and  $B_8$  in NDR renormalization scheme at matching scale  $\mu a = 1$ .

	$B_K$		$B_7$	$B_8$	
	$(p=0)$	$(p=2)$ subtr.			
$CC$	0.92(1)	0.93(2)	0.86(1)	0.94(1)	
$CS$	0.83(1)	0.85(2)	0.82(1)	0.94(1)	
$CU_1$	0.81(1)	0.82(2)	0.81(1)	0.94(1)	
$CU_2$	0.80(1)	0.80(3)	0.81(1)	0.94(1)	
$CU_3$	0.79(1)	0.79(4)	0.80(1)	0.93(1)	
$SS$	0.56(0)	0.64(2)	0.69(30)	0.72(1)	0.92(1)
$SU_1$	0.44(0)	0.57(2)	0.69(23)	0.70(0)	0.90(1)
$SU_2$	0.38(1)	0.53(2)	0.68(21)	0.68(0)	0.89(1)
$SU_3$	0.34(1)	0.51(3)	0.67(19)	0.67(1)	0.88(1)
$U_1U_1$	0.24(0)	0.47(2)	0.68(16)	0.66(0)	0.87(1)
$U_1U_2$	0.11(1)	0.41(3)	0.68(14)	0.64(0)	0.86(1)
$U_1U_3$	0.00(1)	0.36(3)	0.66(12)	0.63(0)	0.84(1)
$U_2U_2$	-0.09(1)	0.33(4)	0.67(11)	0.62(0)	0.84(1)
$U_2U_3$	-0.29(1)	0.26(5)	0.65(10)	0.60(0)	0.82(1)
$U_3U_3$	-0.60(2)	0.14(7)	0.63(09)	0.58(1)	0.80(1)

**$B_7$  and  $B_8$ :** The chiral expansion is similar to Eq. 5 with all 6 coefficients containing artifacts and physical pieces. Ignoring the artifacts we get  $B_7(NDR, 1/a) = 0.60(1)$  and  $B_8(NDR, 1/a) = 0.81(1)$  or with 2-loop running  $B_7(NDR, 2 \text{ GeV}) = 0.59(1)$  and  $B_8(NDR, 2 \text{ GeV}) = 0.81(1)$ . (We find that  $B_8$  is very insensitive to changes in  $\mu$  as the running of the matrix element is almost completely canceled by that of its vacuum saturation approximation, while in the case of  $B_7$  the two add.) Our estimate of  $B_8$  is smaller than that used in the Standard Model analysis of  $e'/\epsilon$  [15]. Since a smaller  $B_8$  means larger  $e'/\epsilon$ , the calculation of  $B_8$  is important phenomenologically. Work is in progress to understand and remove various lattice artifacts and make our estimate more reliable.

## REFERENCES

1. T. Bhattacharya, et al., LA-UR-95-2354.
2. T. Bhattacharya, R. Gupta, LA-UR-95-2355.
3. Bhattacharya, Gupta, LA-UR-95-4222.
4. T. Bhattacharya, R. Gupta, Nucl. Phys. B (PS) 42 (1995) 935.
5. T. Bhattacharya, R. Gupta, in preparation.
6. P. Lepage and P. Mackenzie, Phys. Rev. D48



- (1993) 2250.
7. S. Sharpe, Phys. Rev. D41 (1990) 3233, Phys. Rev. D46 (1992) 3146; J. Labrenz, S. Sharpe, Nucl. Phys. B (PS) 34 (1994) 335.
  8. C. Bernard and M. Golterman, Phys. Rev. D46 (1992) 853.
  9. R. Gupta, Nucl. Phys. B (PS) 42 (1995) 85.
  10. F. Butler, et al., Nucl. Phys. B421 (1994) 217.
  11. C. Allton, et al., Nucl. Phys. B (PS) 34 (1994) 456, and private communications.
  12. S. Hashimoto, et al., hep-lat/9510033.
  13. S. Sharpe, Nucl. Phys. B (PS) 34 (1994) 403.
  14. S. Aoki, et al., hep-lat/9510012.
  15. M. Ciuchini, et al., Z. Phys. C68 (1995) 239.